CZECH TECHNICAL UNIVERSITY IN PRAGUE

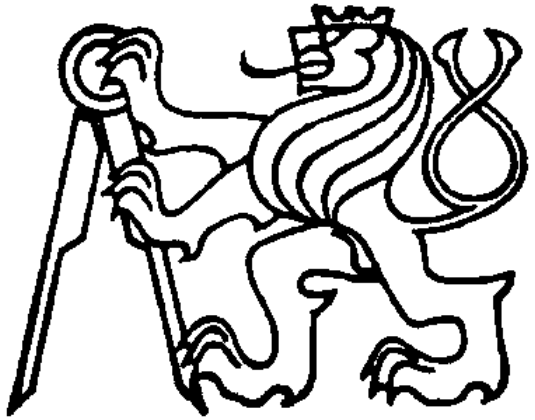

DOCTORAL THESIS STATEMENT

Czech Technical University in Prague

Faculty of Electrical Engineering

Department of Telecommunication Engineering

Ing. Petra Píšová

Determination of the Actual User's Position in Urban Environments Using GNSS Multipath Propagation Model

Ph.D. Programme: Electrical Engineering and Information Technology

Branch of study: Telecommunication Engineering

Doctoral thesis statement for obtaining the academic title of “Doctor”, abbreviated to “Ph.D.”

Prague, February 2015

of individual satellites acquired from the navigation message, and assumed position of the user.

Finding a novel method of the determination of the actual user position based on the previous model.

It is evident that a crucial prerequisite was creating a digital terrain model related to the position of the satellites and determining the reflections of their signals in the defined position of the user. And it is precisely this condition, i.e. creating the model and necessary algorithms, what is the focal point of my dissertation thesis.

The dissertation research also constitutes the material for the patent application entitled “Method of determining the actual position of a user of the GNSS in complicated environments and a system for implementing this method.”

RÉSUMÉ

Disertační práce se zabývá odrazy signálů GNSS (Global Navigation Satellite System - Globální navigační satelitní systémy), které deformují skutečnou polohu uživatele, a metodami vedoucími k jejich potlačení, nebo využití. Hlavní náplní práce bylo:

Poskytnout teoretický přehled metod vedoucích k potlačení vlivu nežádoucích signálů.

Nalézt a odvodit postup pro modelovaní složitého prostředí pomocí inteligentní mapy.

Návrh nového modelu k detekci vícecestného šíření signálu v dynamickém prostředí pomocí ray tracing algoritmu, 3D modelu budov, známých poloh jednotlivých družic získaných z navigační zprávy a předpokládané polohy uživatele.

Nalézt nový způsob zjištěni skutečné polohy uživatele na základě předchozího modelu.

Je zřejmé, že klíčovou potřebou bylo vytvoření digitálního modelu terénu ve vazbě na polohu družic a stanovení odrazů jejich signálů pro definovanou polohu uživatele. Na tento cíl, tedy vytvoření modelu a potřebných algoritmů, jsem soustředila těžiště disertační práce. Ostatní kroky jsou již standardní inženýrskou činností. Je skutečností, že pro výpočet je nutný značný výpočetní výkon – výpočet může na běžném PC trvat řádově jednotky hodin, ale náprava nemusí být v tom, že budeme požadovat tento výkon přímo na místě, resp. čekat až procesory tohoto výkonu budou běžně dostupné, ale požadovaná data můžeme odeslat do cloudu, kde tento výkon již může být připraven, pomocí komunikační linky.

Řešení disertační práce je současně i podkladem pro přihlášku vynálezu s názvem : „Způsob stanovení skutečné polohy uživatele GNSS ve složitém prostředí a systém k provádění tohoto způsobu“.

2. Other publications

Journals (Impact)

None

Journals (Reviewed)

None

Conference Proceedings

- Vojtěch, L., Píšová, P.: RFID - A Technology for Radio Frequency Contactless Identification. In *Moderní trendy v digitálních přenosových systémech*. Praha: Česká elektrotechnická společnost, 2007, s. 39-42. ISBN 978-80-02-01922-0.

- Píšová, P. - Tomešová, K. - Plotnikova, M. - Zikmund, M.: Communication and Nanotechnology. In *13th International Student Conference on Electrical Engineering*. Prague: CTU, Faculty of Electrical Engineering, 2009, p. C6.

Grants

- Krejčí, J.: Suitable Methods for Evaluation of Image Signal Quality in Digital TV Systems. 09--09, FRV 1378G1, 2009.

- Šafránek, M.: Innovation of Laboratory Exercises in the Subject 'Switching Systems'. 10--10, FRV G1 2219, 2010.

- Šafránek, M.: Communication and automatic data collecting system with a use of satellite network, high reliability and low power consumption for Czech Antarctic base station. 10--11, SGS SGS10/183/OHK3/2T/13, 2010.

- Zeman, T.: Modern Coding Methods. 10--10, FRV F1a 1752, 2010

SUMMARY

This dissertation thesis deals with the problem of reflected GNSS (Global Navigation Satellite System) signals, which are responsible for distorting the information on the actual user position, and with methods on their mitigation and utilization. It was focused mainly on:

Presenting a theoretical overview of the methods of unwanted signals mitigation.

Defining and deriving a technique to model complex environments using an intelligent map.

Proposing a new model of multipath signal propagation in a dynamic environment using the ray-tracing algorithm, 3D building model, known positions

The doctoral thesis was produced in combined manner Ph.D. study at the department of Telecommunication Engineering of the Faculty of Electrical Engineering of the CTU in Prague.

Candidate: Ing. Petra Píšová
Department of Telecommunication Engineering
Faculty of Electrical Engineering of the CTU in Prague
Technická 2, 166 27 Prague 6

Supervisor: Doc. Ing. Jiří Chod, CSc.
Department of Telecommunication Engineering
Faculty of Electrical Engineering of the CTU in Prague
Technická 2, 166 27 Prague 6

Opponents: .....

.....

.....

The doctoral thesis statement was distributed on: .....

The defence of the doctoral thesis will be held on.....at .....a.m./p.m. before the Board for the Defence of the Doctoral Thesis in the branch of study Telecommunication Engineering in the meeting room No. .....of the Faculty of Electrical Engineering of the CTU in Prague.

Those interested may get acquainted with the doctoral thesis concerned at the Dean Office of the Faculty of Electrical Engineering of the CTU in Prague, at the Department for Science and Research, Technická 2, Praha 6.

.....

Chairman of the Board for the Defence of the Doctoral Thesis in the branch of study Telecommunication Engineering Faculty of Electrical Engineering of the CTU in Prague, Technická 2, 166 27 Prague 6.

1. CURRENT SITUATION OF THE STUDIED PROBLEM

It is well known that multipath is a phenomenon that accounts for a dominant source of error in precise global positioning. In dynamic urban environment, it changes rapidly so it is difficult to detect, predict, and control.

Generally, direct (or line-of-sight) signal is normally the most wanted signal. Nevertheless, signals can also arrive at the receiver via a number of different paths that may occur between the satellite and the receiver. These paths are results of reflections and diffractions from buildings of different heights, structures, and materials – reducing the number of visible satellites and thus increasing the presence of multipath.

Typically, an antenna receives the direct signal and one or more of its reflections. The reflected signal is usually a weaker version of the direct signal which takes more time to reach the receiver than the direct signal. This path delay, or rather this difference between the length of the path taken by the reflected signal and the direct signal itself (between the satellite and the receiver) causes an important pseudorange measurement error.

It is difficult to mitigate the multipath by models, because it depends strongly on users' local environment – the influence of given signal and receiver parameters on the actual multipath error depends on various factors.

Analysing different combinations of Global Navigation Satellite Systems (GNSS) constellations promises more considerable improvements than mere analysing data from a single GNSS constellation. There are several satellite systems in operation today, such as the United States NAVSTAR Global Positioning System (GPS) or the Russian GLONASS (Global'naya Navigatsionnaya Sputnikovaya Sistema). Chinese Compass navigation system and the European Union's Galileo navigation system are currently under construction.

Three-dimensional (3D) reconstruction and texturing of buildings is becoming increasingly important for a number of applications and has been a topic of active research in recent years. As 3D building models are becoming more geometrically accurate, they can be regarded as new true data sources which can improve positioning accuracy in urban canyons.

Therefore, one promising solution is to use known positions of the satellites extracted from a navigation message in combination with 3D building models and known position of the user. These quantities may help to calculate the path lengths of direct signals and even path delays of reflected signals and thus to predict blockage and reflection of GNSS signals. This approach can be then used to estimate the subject's unknown position while moving in the same environment.

Influence of given signal and receiver parameters on the actual multipath error depends on various factors [1]: code chipping rate; signal-type modulation; pre-correlation bandwidth and filter characteristics; number of received multipath

Patent

- Pisova, P., Chod, J.: Patent application PV 2015: "Způsob stanovení skutečné polohy uživatele GNSS ve složitém prostředí a systém k provádění tohoto způsobu" (in Czech). "Method of determining the actual position of a user of the GNSS in complicated environments and a system for implementing this method" (in English).

Conference Proceedings

- Chod, J., Píšová, P., Koláčný, R., Šafránek, M.: HW a SW of the Navigation Centre for Blind Persons. In *Sborník přednášek konference NavAge 08.* Praha: Technology&Prosperity, 2008. ISBN 978-80-87205-00-6.

- Chod, J., Píšová, P., Šafránek, M.: Navigace nevidomých – 2008. *EMTECH 2008.* Praha: ČVUT v Praze, FEL, 2008. ISBN 978-80-01-04198-7.

- Chod, J., Píšová, P., Šafránek, M., Koláčný, R.: Projekt navigace nevidomých – 2008. *MonAMI* - IST – 5 – 035147. Košice: Technical University of Košice, 2008.

- Píšová, P.: Global Navigation Satellite Systems for Mobile Communication. In *Applied Electronic 2010.* Pilsen: University of West Bohemia, 2010, p. 261-264. ISSN 1803-7232. ISBN 978-80-7043-865-7.

- Píšová, P., Kalfus, R., Chod, J.: Detection of Reflected GPS Signals. In *13th International Conference on Research in Telecommunication Technologies 2011*. Brno: Vysoké učení technické v Brně, Fakulta elektrotechniky a komunikačních technologií, 2011, p. II-35-II-39. ISBN 978-80- 214-4283-2.

Grants

- Chod, J.: Innovation of Laboratory Projects Assignments for the Subject MKS. 08--08, FRV 2294 F1a, 2008.

- Píšová, P.: Modernization of Laboratory Exercises in the Field of Navigation Systems. 11--11, FRV G1 2107, 2011.

- Chod, J.: Advanced Navigation of the Blind.13--15, TA03011396, 2014.

[16] Sunday, D. *About Planes and Distance of a Point to a Plane.* 2001 [online]. Available: http://www.geometry algorithms.com

[17] Pany, T. *Navigation Signal Processing for GNSS Software Receivers.* Norwood, MA: Artech House, 2010. ISBN 978-1-60807-027-5.

[18] Prasad, R. and M. Ruggieri. *Applied Satellite Navigation Using GPS, GALILEO and Augmentation Systems.* Boston: Artech House, 2005. ISBN 1-58053-814-2.

[19] El-Rabbany, A. *Introduction to GPS. The Global Positioning System.* 2nd ed. Norwood, MA: Artech House, 2006. ISBN 978-1-59693-016-2.

Software

[S1] Google Earth (Google).

URL: **http://earth.google.com**

[S2] 3D Ripper DX v1.8 (Roman Lut).

URL: **http://3d-ripper-dx.software.informer.com**

[S3] Autodesk 3ds Max 2011 (Autodesk).

URL: **http://www.autodesk.com/education/free-software/3ds-max**

[S4] Matlab 7.11.0 (Mathworks).

URL: **http://www.mathworks.com/**

[S5] Mathematica 8 (Wolfram)

URL: **http://www.wolfram.com/products/?source=nav**

PUBLICATIONS

1. Publications related to thesis

Journals (Impact)

None

Journals (Reviewed)

Planned:

- Pisova, P., Chod, J.: Detection of GNSS signals propagation in urban canyons using 3D city models. In *Advances in Electrical and Electronic Engineering*. Article will be published within the next issue (March 2015).

signals; relative power of multipath signals; path-delay; chip spacing between correlators; type of discriminator and algorithm used for code and carrier frequency tracking.

Different techniques exist to mitigate the effect of multipath signals. In general, they can be grouped into three main categories: antenna-based, receiver-based, and post receiver- based techniques. Many are used in combination [2].

Antenna-based mitigation techniques

As mentioned above, GNSS signals are right-hand circularly polarized (RHCP), while most reflected signals show left-handed circular polarization (LHCP) or mixed polarization. The signal, however, remains RHCP when the angle of incidence is greater than the Brewster's angle. Brewster's angle varies with different reflective surfaces [3]. A RHCP antenna is able to supress the LHCP reflection quite effectively too and minimize (but not entirely remove) the multipath reflection error.

Therefore, the principle applied in GNSS antennas means increasing the sensitivity for RHCP and simultaneously decreasing the sensitivity of LHCP signals: A well-designed GNSS antenna is at least 10 decibels more sensitive to RHCP signals than LHCP signals at normal incidence in order to decrease the magnitude of the code and carrier tracking errors due to multipath appearance. The exception is the case of low elevation signals, for which the antenna has very little polarization discrimination. To attenuate low and negative elevation signals, modern design uses variable choke-ring antennas (depending on space permits) [2].

A space-effective alternative is the use of the dual-polarization antenna technique which correlates the right hand circularly polarized (RHCP) and left hand circularly polarized (LHCP) outputs separately. If an LHCP C/N_0 is larger than the corresponding RHCP C/N_0, the multipath interference is detected. This is not effective for low elevation signals [4].

Another technique is the use of a GNSS antenna array to estimate the angle of arrival (AOA) of incoming GNSS signals [2]. For multipath and directly received signals determination, measured lines of sight are compared with data predicted from the satellite ephemeris. This method is used for detecting strong multipath interference.

An advanced method is special processing that uses directive antenna arrays to provide required directive pattern with high gain in the direction of the direct signal and attenuation from directions of reflected signals [5]. Directive antennas are not affordable for most civilian applications because they are usually physically large and heavy [2].

Receiver-based mitigation techniques

There are many techniques to mitigate the effects of multipath on pseudorange measurements by increasing the resolution of the receiver's code discriminator, and thus separating the direct signal from the reflected signal components [2].

Examples of recently developed in-receiver multipath mitigation techniques are:

- narrow correlator;
- double-delta discriminator;
- gated and high resolution correlator;
- multipath-estimating delay lock look (MEDLL);
- vision correlator;
- strobe and edge correlator;
- enhanced strobe correlator;
- multipath elimination technology (MET);
- multipath mitigation technology (MMT);
- maximum likelihood (ML) estimator;
- pulse aperture correlator (PAC;
- early1/early2 (E1/E2) tracking technique.

Superior methods like MEDLL, MMT, and VC rely on maximum likelihood (ML) estimation principles. However, they are typically complex and difficult to implement as they require cross-correlation function for each reflected path with multiple correlators to measure the received signal and to process these measurements with complex algorithms [1].

Post receiver-based mitigation techniques

Multipath effects on code and phase measurements differ extensively. Multipath also creates different errors on different frequencies, it can be therefore detected and mitigated by comparing different measurements of signals on different frequencies from the same satellite [6] – an example is carrier smoothing to reduce code multipath errors for dynamic applications [2].

Another method is signal selection based on consistency checking: the position is computed using measurements from different satellites that are compared with each other to identify reflected signals. The same principle is used for fault detection in receiver autonomous integrity monitoring (RAIM) where algorithms require at least five visible satellites to detect the presence of a large position error [7].

High performance positioning is also achieved by using Kalman filter where inconsistent measurements are determined by using information from previous epochs.

Further information on multipath interference may be found in standard GNSS books [2].

and Multipath Mitigation in Dense Urban Areas. Proceedings of the 26th International Technical Meeting of The Satellite Division of the Institute of Navigation (ION GNSS 2013). (pp.3231-3247). Manassas,US The Institute of Navigation, 2013.

[5] Grewal, M.S., L.R. Weil and A.P. Andrews. *Global Positioning Systems, Inertial Navigation, and Integration*. John Wiley & Sons, Inc., 2007, pp. 144-194, ISBN-13 978-0-470-04190-1.

[6] Lau, L. and P. Cross. *Investigations into Phase Multipath Mitigation Techniques for High Precision Positioning in Difficult Environments.* Journal of Navigation, 2007, Vol. 60, No. 1, pp. 95−105.

[7] Kaplan, E.D and Ch. J. Hegarty. *Understanding GPS - Principles and Applications*. 2nd ed. Artech House, 1996. ISBN 0-89006-793-7.

[8] Brenner C. *Building reconstruction from images and laser scanning.* Inter. J. Appl. Earth Obs. Geoinf. 2005; 6:187–198.

[9] Umesh Chandra Pati. 3-*D Surface Geometry and Reconstruction: Developing Concepts and Applications*, (National Institute of Technology, Rourkela, India), Publisher: IGI Global; 1 edition (February 29, 2012), ISBN-10: 1466601132.

[10] Neutens, T. and P. De Maeyer. *Developments in 3D Geo-Information Sciences*. Springer, Berlin, 2010. ISBN 978-3-642-04790-9.

[11] IGS Product Availability: *GPS ephemeris, clock and earth orientation solutions.* 2014 [online]. Available: http://igscb.jpl.nasa.gov/components/prods_cb.html

[12] Leduc, S. A. *Linear Algebra* (Cliffs Quick Review), Cliffs Notes, 1996 [online]. ISBN 978-0-8220-5331-6. Available: http://www.cliffsnotes.com/math/algebra/linear-algebra/real-euclidean-vector-spaces/linear-independence

[13] Borre, K., D. M. Akos, N. Bertelsen, P. Rinder and S. H. Jensen. *A Software-Defined GPS and Galileo Receiver. A Single-Frequency Approach.* Series: Applied and Numerical Harmonic Analysis. Boston: Birkhäuser, 2007. ISBN 978-0-8176-4540-3.

[14] *The Feynman Lectures on Physics, Volume I* [online]. 2013 Interference. Diffraction. Radiation Damping. Light Scattering. Polarization. Modes. Available at: http://www.feynmanlectures.caltech.edu/.

[15] IGS Product Availability: *GPS ephemeris, clock and earth orientation solutions.* 2014 [online]. Available: http://igscb.jpl.nasa.gov/components/prods_cb.html

position of the receiver, and known position of GNSS satellites extracted from the navigation message.

There is no direct way to export the geometry with textures and coordinates mapped automatically. Therefore a new technique to model complex environments using an intelligent map was defined and derived.

For each satellite, the algorithm determines whether the signal has arrived at the receiver through a direct path or through multipath reflections. Furthermore, the algorithm is able to estimate the number of multipath reflections and their coordinate data within the proposed simulation system. With this information, the distance the signal travelled to the receiver, as well as its the transit time, are calculated.

The model is established and validated using experimental as well as real data. It is specially designed for complex environments and situations where positioning with highest accuracy is required – a typical example is navigation for the visually impaired.

This approach can be then used to determine the user's position in dynamic propagation environment thanks to the fact that if it is possible to calculate the total propagation path length of the GNSS signals – using intelligent maps and other data – then it is also possible to perform the order of operations in reverse and thus to determine the actual, unknown position of the user.

Based on the research results presented in this work, detection of GNSS signals propagation in urban environments can improve accuracy of the pedestrian positioning. The data processing algorithm requires sufficient computational power. Therefore, it is expected the data will be sent to the cloud for faster computation.

In future work, an investigation in the multi-constellation GNSS area and right selection of direct/multipath signals using the method presented, combined with other options – e.g. using antennas capable of receiving only phase undistorted GNSS signals, or cameras able to determine which part of the sky is uninterrupted by objects – seems to be interesting.

BIBLIOGRAPHY

[1] Sahmoudi, M. Landry, R. *Probabilities and Multipath. Mitigation Techniques Using Maximum-Likelihood Principles.* InsideGNSS [online]. Technical Article, November/December 2008.

[2] Petovello, M.and P. Groves. *Multipath vs. NLOS signals.* InsideGNSS [online]. GNSS Solutions, November/December 2013.

[3] GROVES, P. D. *Principles of GNSS, Inertial, and Multi-Sensor Integrated Navigation Systems (GNSS Technology and Applications).* 2nd ed. Boston: Artech House, 2013. ISBN 978-1-60807-005-3.

[4] Groves, P. D., Z. Jiang, M. Rudi, P. Strode. *A Portfolio Approach to NLOS*

2. AIMS OF THE DOCTORAL THESIS

Global navigation satellite systems (GNSS) have been in operation for several decades. They affect virtually all areas of human activity. Thanks to augmentation systems (involving correction of signal propagation in the ionosphere and differential measurements at referential points), their accuracy – typically about 1 m – is satisfactory under usual conditions of their applications. The problem arises when the position needs to be determined in complex environments, such as narrow town streets, mountain valleys etc., where the signal tends to be reflected from various obstacles. This causes signal delays, thereby distorting user positioning accuracy. Depending on the nature of the environment, the deviation may amount up to tens or hundreds of meters. This system deficiency is not necessarily fatal in today's situation when cars are operated by drivers. In this case, some deficiencies can be corrected, e.g. by software combination of the data with the information on a navigation route and by estimation of the real position by a driver. However, the situation changes dramatically in case of unmanned, self-driving vehicles. Although these are not very common yet, this era is fast approaching. This problem is also very pressing in other areas where the exact position needs to be determined, such as in precise data processing within the navigation for the visually impaired.

There are many methods to counter these problems. The simplest approach is based on the knowledge of the fact that polarization of a GNSS signal changes upon reflection (from right-handed to left-handed and vice versa). There is thus an option to consider only those signals which did not undergo this change. For this purpose, antennas suppressing unwanted (i.e. unsuitably polarized) signals may be used. Similarly, it is possible to determine the actual segment of the sky situated above a receiver which contains only directly "visible" satellites. This may be done using intelligent maps which contain data on the location and height of surrounding objects. While the first method is already commonly available, the other – map-based computation – is currently not widely used as it is very demanding of computing power of the receiver processor. Moreover, the number of satellites situated in direct line of sight is usually not sufficient so the position cannot be determined with satisfactory accuracy.

I have decided to design a new technique which is based on the fact that intelligent maps (i.e. those which contain information on the height of surrounding objects and possibly other relevant data, such as the nature and structure of the surface) are relatively easily available today and they can be used to determine the actual position by calculating signal reflections and their comparison with the data measured by a navigation receiver.

The main task is thus finding a computing model which would be able to provide the information on reflected signals from navigation satellites (because their position at any point in time is known with sufficient accuracy). If we know the expected situation of direct versus reflected signals at a defined location, then it is

also possible to reverse the procedure and to look for the actual position of a GNSS user by means of the comparison of the measured and calculated data. This can be done using the interval halving method in several (typically three to five) steps until the difference between the calculated and measured data is acceptable.

The dissertation objectives are thus as follows:

1. An analysis of the environment and the movement of a GNSS user within the area of interest.
2. Determining the anticipated route of the GNSS user, including the definition of deviation tolerance intervals.
3. In case of a mismatch between the position measured by the GNSS and the anticipated route, determining the number of directly visible satellites. If the number of satellites is not sufficient (fewer than four), determining the starting point and the endpoint of the route in the area of interest.
4. Computation of a 3D-object model using an intelligent map, taking into ac-count the data on positions of all available satellites situated above the horizon.
5. Setting the beginning of the computation of signals and their reflections to the midpoint of the route (a point halfway between the starting point and the endpoint as defined in point 3).
6. Computation of the signals and their reflections using the model.
7. Depending on the contrast between the position computed and data meas-ured, a consequent decision which half of the route is relevant, then moving the next step of the computation to the midpoint of this segment.
8. Another round of signal computation for the new position and displaying the result (i.e. repeating point 6).
9. Repeating point 7 in subsequent steps until the difference between the meas-ured and computed positions lies within the desired tolerance interval.
10. Marking the last computed position as the actual position.

It is evident that a crucial prerequisite is creating a digital terrain model related to the position of the satellites and determining the reflections of their signals in the defined position of the user. And it is precisely this condition, i.e. creating the model and necessary algorithms, what is the focal point of my dissertation thesis.

3. 3D ENVIRONMENT MODEL

3D reconstruction and texturing of buildings has become increasingly important for a number of applications and has been an active research topic in recent years. There is a variety of approaches with different resolutions, levels of accuracy, methods, completion times, stages and costs (e.g. laser scanners, photogrammetric approach). For more, see e.g. [8], [9].

Table 5. 4 shows the result of one reflection.

Satellite ID 5	
Direct Path:	No
Number of signals with a single reflection:	1
Reflection point coordinate data (Xm, Ym, Zm):	1.0e+002 * [-1.8066, -0.6410, -0.0499]

Table 5. 4 Results shown for GPS, Satellite ID 5

From the knowledge of reflection points coordinates, the distance from the satellite to the receiver is computed, equation (4. 20), equation (4. 23). Computation time increases extensively with the amount of 3D map information, and number of satellites and receivers.

C – Detection of the User's Pseudo-Position

Computed data are forwarded to the receiver - based on the results of the ray-tracing algorithm, the receiver computes its new position which is different from the originally known position of the user.

Depending on the difference between the position computed and data measured, a consequent decision which half of the route is relevant, moving the next step of the computation to the midpoint of this segment.

Another round of signal computation for the new position is done until the difference between the measured and computed position lies within the desired tolerance interval. The last computed position is the actual position.

These steps account for standard engineering tasks. It is true that this sort of computation is dependent on considerable computing power: The completion of the above mentioned calculation may require up to several hours of time using a standard PC. However, the necessary solution does not require having this kind of computer power on the spot or waiting until the processors capable of this output are available: The data may be sent to the cloud via a line of communication where this sort of power may be at hand.

6. CONCLUSION

The presence of reflected and diffracted signals in urban environments seriously degrades GNSS positioning in terms of accuracy, integrity, and precision. Possible combinations of GNSS constellations promise better results with respect to GPS only. Although the current situation only allows using GPS and GLONASS to the full extent, additional satellites of Galileo and Compass will offer significantly improved GNSS performance and availability in the near future.

Within this research, a new ray-tracing model for simulation of GNSS signals reception in urban canyons was designed. To investigate whether GNSS signals have arrived at a receiver directly or through reflections, the ray-tracing algorithm was introduced based on information obtained from 3D buildings model, assumed

SV Id	x-axis (km)	y-axis (km)	z-axis (km)
1	-13588.7	22126.96	5159.559
2	16473.63	-1019.71	-20414
3	-17858.5	1989.12	19045.99
4	4294.17	20627.37	-16296.3
5	26516.43	-1724.24	-2094.13
7	-5040.23	24550.11	8313.925
8	-1615.86	21746.78	14861.25
10	19225.86	9773.089	-16112.9

Table 5. 2 Examples of satellite coordinates obtained from the navigation message (1.12.2014 – 6pm)

B – Detection of GNSS signals propagation

The model described in previous section is evaluated using the multipath detection algorithm based on an assumed position of the receiver, digital 3D maps information, and known positions of GNSS satellites, chapter 4.

As a result, a list of all direct paths and possible reflections examples for a given satellite and the receiver along with coordinate data of reflected points is displayed – the example below:

Table 5. 3 shows the result of two reflections.

Satellite ID 7	
Direct Path:	No
Number of signals with a single reflection:	0
Number of signals with two reflections:	3
Signal 1	
Reflection point coordinate data (X1m, Y1m, Z1m):	1.0e+011 * [3.7131, -1.9701, 0.1399]
Reflection point coordinate data (X2m, Y2m, Z2m):	1.0e+002 * [-1.5763, -0.7414, -0.0099]
Signal 2	
Reflection point coordinate data (X1m, Y1m, Z1m):	1.0e+007 * [2.0910, -1.1095, 0.2041]
Reflection point coordinate data (X2m, Y2m, Z2m):	1.0e+012 * [-5.4743, -6.2745, -0.7086]
Signal 3	
Reflection point coordinate data (X1m, Y1m, Z1m):	1.0e+002 * [-1.4315, -0.6138, -0.0076]
Reflection point coordinate data (X2m, Y2m, Z2m):	1.0e+002 * [-1.4427, -0.5883, -0.0084]

Table 5. 3 Results shown for GPS, Satellite ID 7

Moreover, as 3D building models are becoming more geometrically accurate, they can truly be regarded as a new data source to improve the positioning accuracy in urban canyons. Research done in the dissertation focuses on these models to evaluate GNSS positioning performance with 3D ray tracing techniques. This can be achieved using satellite visibility and geometry predictions for any given location compared with measured satellite visibility to determine the user's current position.

This chapter deals with obtaining 3D geometry data from a real environment, extracting them into 3D modelling software, determining current satellites visibility above the user's receiver, and transforming their coordinates into the same units.

3D Data Visualization

The most known 3D Geospatial Browser is Google Earth. Digital model or 3D representation of a terrain's surface is available in a Digital Elevation Model (DEM – a type of raster Geographic Information System GIS layer) format, albeit not that accurate for many areas [10].

There are two distinct methods to represent the building geometries [61]. The first method defines a base polygon that corresponds to the floor plan of the building and extends it to the height of the building. The other method uses multiple polygons which allow more detailed geometrical representation of the building elements.

Other well-known 3D Geospatial Browsers are e.g. Microsoft Virtual Earth or NASA World Wind.

3D Data Extraction

There is no direct way to export the geometry with textures and coordinates mapped automatically. For my purpose, I used 3D Ripper DX to capture, import, and export given urban environment from Google Earth into Autodesk 3ds Max.

Capturing Google Earth Geometry - Steps to follow:

Download and run Google Earth [S1], go to Tools > Options and set the Graphics Mode to DirectX. Leave all other settings at default. Apply changes and close it.

Download and run 3D Ripper DX [S2], tick checkbox and copy and paste Autodesk 3D Max 2011 path manually. Select googleearth.exe path , define Capture key and press the Launch button.

In Google Earth, there is a Ready to capture yellow label displayed in the left corner. Go to the point of destination Click on North button on compass and press the Capture key. Exported data are stored in output directory defined in 3D Ripper DX Options.

Importing / exporting data from Autodesk 3ds Max 2011 - Steps to follow

Download and run Autodesk 3ds Max 2011 [S3]. Import captured data in 3.dr file and change settings to:

- FOV: horizontal (for width) to 60 (defined for Google Earth)
- Monitor aspect ratio (for Google Earth): 1.58 (image size1025:646)

Export data into .obj file - the building layout is considered to be made up of triangles put together.

Satellite Coordinates Extraction

The information about which satellite is visible for a certain receiver in a 3D city model at a certain time is found in GNSS almanac data [11]. Satellite coordinates are computed in Earth-centred, Earth-fixed (ECEF) WGS-84 coordinates.

Satellite Coordinates Transformation

The position of the receiver is reported in mapping coordinates $(X_m, Y_m, Z_m$ – the same coordinate system when extracting building geometry from Google Earth). The satellite position coordinates are in different units.

The transfer matrix between these two coordinate systems is as follows:

$$\mathbf{M}_{\mathbf{ECEF\_MC}} = \begin{bmatrix} -\sin(\beta) & \cos(\beta) & 0 \\ -\cos\beta * \sin\alpha & -\sin(\beta) * \sin(\alpha) & \cos(\alpha) \\ \cos(\alpha) * \cos(\beta) & \cos(\alpha) * \sin(\beta) & \sin(\alpha) \end{bmatrix}, \quad (3.\ 1)$$

where α and β respectively represent latitude (N) and longitude (E) coordinates converted to radians.

4. MULTIPATH DETECTION MODEL FOR DYNAMIC PROPAGATION ENVIRONMENTS

In the following, the proposed multipath detection model for dynamic propagation environments is presented.

Generally, direct (i.e. line-of-sight, LOS) signal is normally the most wanted signal. Nevertheless signals can also arrive at a receiver via a number of different paths that may occur between a satellite and a receiver. These paths are results of reflections and diffractions from buildings, water, ground etc.

To investigate whether GNSS signals have arrived at a receiver directly or through reflections, the ray-tracing algorithm is introduced based on information obtained from 3D buildings model, assumed position of the receiver, and known position of GNSS satellites extracted from the navigation message.

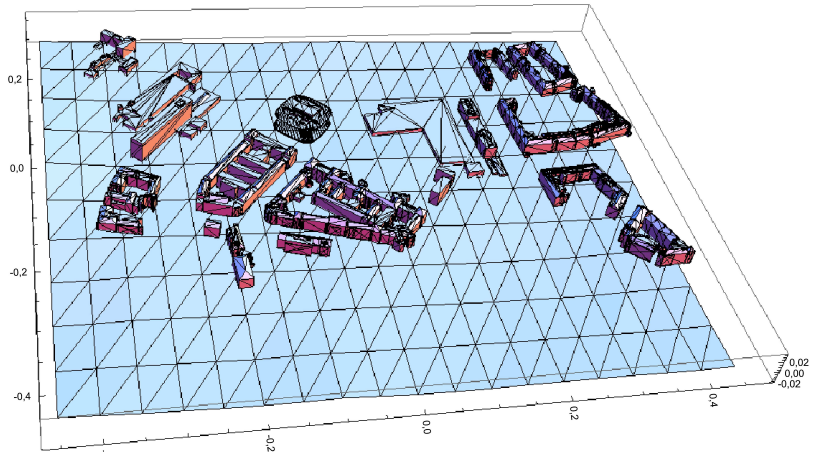

Figure 5. 2 Street model of Prague in .obj file

The building (or street) layout is made up of triangles ABC which are imported into Matlab in the form of .cvs files. In the Table 5. 1 below, examples of triangle coordinates of Studentská street are shown.

Ax	Ay	Az	Bx	By	Bz	Cx	Cy	Cz
0.1086	-0.0365	0.0046	-0.0595	0.0397	0.0076	-0.1086	0.0397	0.0066
-0.1577	-0.0365	0.0036	-0.1086	-0.0365	0.0046	-0.1086	0.0397	0.0066
-0.1531	-0.0749	0.0032	-0.1553	-0.0809	0.003	-0.1553	-0.0809	-0.0112
-0.1531	-0.0749	-0.0119	-0.1531	-0.0749	0.0032	-0.1553	-0.0809	-0.0112
-0.1471	-0.083	-0.0148	-0.1503	-0.0759	-0.0148	-0.1503	-0.0759	-0.0132
-0.1466	-0.084	-0.0151	-0.1466	-0.084	-0.0148	-0.1471	-0.083	-0.0148
-0.1512	-0.0845	-0.0131	-0.1466	-0.084	-0.0148	-0.1466	-0.084	-0.0151
-0.1544	-0.0848	-0.0118	-0.1544	-0.0848	-0.0119	-0.1512	-0.0845	-0.0131
-0.1553	-0.0809	0.003	-0.1544	-0.0848	0.0031	-0.1544	-0.0848	-0.0118
-0.1553	-0.0809	-0.0112	-0.1553	-0.0809	0.003	-0.1544	-0.0848	-0.0118

Table 5. 1 Examples of triangle coordinates, Studentská Street, Prague

Navigation message extraction to obtain satellites coordinates and their transfer into mapping coordinates is done next, the methodology is described in chapter 3. Table 5. 2 shows examples for first 10 satellites.

Depending on the availability of known positions of satellites obtained from navigation messages of different GNSS systems, the multipath signal propagation model is evaluated.

Test measurements were performed in Europe and Asia for GPS, GLONASS, Galileo and Compass. With the fact that the evaluation of the ray-tracing method and simulations is the same for all GNSS systems, further conclusions are concentrated on the GPS, which is the most available GNSS system.

Model 1: Europe, Prague, Studentská street

A – Model preparation

A building block in city model of Prague with variable parameters for street width, street length, and building block parameters with an assumed position of the receiver (50°06'10.01" N, 14°23'24.18" E) was considered.

Figure 5. 1 shows a street as captured in Google Earth, 3D Environment methodology described in chapter 3.

The selected urban environment is captured by 3D Ripper DX and imported into Autodesk 3ds Max 2011 - the geometry data of the street is then exported into .obj file, as described in chapter 3 (Figure 5. 2 shows the Studentská street in .obj file).

Figure 5. 1 Street model of Prague in Google Earth

All MATLAB code ([S4], [S5]) can be found on the supplemented CD attached to the doctoral thesis back cover.

Calculation of Direct Path

Consider **SP** from S (satellite) to P (receiver), and a triangle with vertices A,B,C (obtained from the 3D map), as illustrated in Figure 4.1

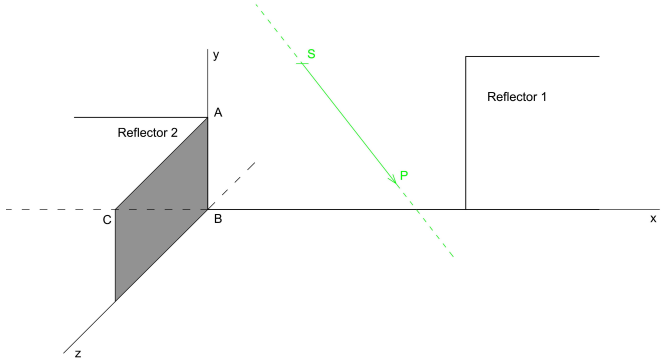

Figure 4. 1 Illustration of GNSS signal – direct path

Linearly independent vectors

To avoid all points (S,P,A,B,C) being on the same line, the algorithm provides an estimate of the number of linearly independent vectors **AB** , **BC** and **SP** . They are linearly independent if none of them can be expressed as a linear combination of the others, otherwise they are dependent and the algorithm does not consider them in further calculations.

Let $A=\{\mathbf{AB},\mathbf{BC},\mathbf{SP}\}$ be a collection of vectors from R^3. Then the vectors are said to be linearly independent if [12]:

$$rank(A)=3. \qquad (4.\ 1)$$

Line-of-sight between two points

To get the intersection of the vector **SP** with the $\triangle$ABC, we first determine the intersection of the vector **SP** and the plane ρ ($\triangle$ABC $\in$ ρ). If it does not intersect, then it also does not intersect the $\triangle$ ABC and the time and distance from the satellite to the receiver are calculated from pseudoranges. However, if they do intersect in the point R (reflection), we need to determine if this point is inside the $\triangle$ ABC.

The true geometrical range between satellite k and receiver i can be denoted ρ_i^k [13]:

$$\rho_i^k = \sqrt{(X^k - X_i)^2 + (Y^k - Y_i)^2 + (Z^k - Z_i)^2}\ . \qquad (4.\ 2)$$

A limitation is done to exclude the intersection point R as a part of the ray **SP** ($R \notin \mathbf{SP}$).

Intersection of a ray with a plane

A plane is defined by three non-collinear points (three points not on a line) $A,B,C \in R^3$. These three points define two distinct vectors **AB** and **AC**. The △ABC lies in the plane ρ through A with normal vector **w** [14]:

$$\mathbf{w} = \mathbf{AB} \times \mathbf{AC}. \qquad (4.\ 3)$$

Then the parametric plane equation through a point is:

$$\mathbf{R} = \mathbf{A} + (\mathbf{B} - \mathbf{A}) \cdot s + (\mathbf{C} - \mathbf{A}) \cdot u, \qquad (4.\ 4)$$

where $s,u \in R$.

The parametric equation of a ray that passes through a point is:

$$\mathbf{R} = \mathbf{P} + (\mathbf{P} - \mathbf{S}) \cdot t, \qquad (4.\ 5)$$

where $t \in R$.

By inserting equation (4. 3) to equation (4. 4), we get the solution to s,t,u:

$$\mathbf{M}_{\mathbf{t,s,u}} = \begin{bmatrix} S_x - P_x & B_x - A_x & C_x - A_x & P_x - A_x \\ S_y - P_y & B_y - A_y & C_y - A_y & P_y - A_y \\ S_z - P_z & B_z - A_z & C_z - A_z & P_z - A_z \end{bmatrix}. \qquad (4.\ 6)$$

By substituting the solution of equation (4. 6) into equation (4. 4) or equation (4. 5), we get the parametric coordinates of the intersection point R in the plane.

Calculation of Single Reflection

Further, different models of reflection are considered. First, a single reflection model is described, as illustrated in Figure 4. 2.

Intersection of a point and a plane

The basic criteria to determine whether a point R_1 lies inside a triangle defined with vertices A, B, C or not is as [14], [1562]:

$$\alpha_1 + \alpha_2 + \alpha_3 = 1\ , \qquad (4.\ 7)$$

$$\alpha_1, \alpha_2, \alpha_3 \geq 0\ , \qquad (4.\ 8)$$

$$\alpha_1 \mathbf{A} + \alpha_2 \mathbf{B} + \alpha_3 \mathbf{C} = \mathbf{R_1}\ , \qquad (4.\ 9)$$

From the knowledge that GNSS signals travel at the speed of light and the known distance to the receiver, we can calculate the time the signal took to reach the receiver.

Detection of a User's Position

It is evident that if it is possible to calculate the total propagation path length of the GNSS signals – using intelligent maps and other data – then it is also possible to perform the order of operations in reverse and thus to determine the actual, unknown position of the user.

The principle is described as a sequence of following steps:

- determining the number of satellites visible using a combination of intelligent maps and known position of the subject;
- performing calculations to determine the position (the position in a presumed region) if the number of satellites that are in direct line-of-sight is greater than or equal to three;
- based on combination of intelligent maps data (including terrain and buildings height) and measured GNSS data (with known positions of satellites obtained from navigation message) – the final position of the receiver is found;

Typical application of a new method of determining the position is as follows:

The user is equipped with a GNSS receiver able to plan and define the route where he moves along. In a simple environment the position of the user is displayed on the map inside the planned rout. In a complex environment this may not be obvious thanks to the influence of reflections of GNSS signals. In the case the position of the user (measured data from the GNSS receiver) is displayed outside the planned route, it is necessary to define his true position. This means to find such a point in the specified interval (defined by his last known position and the place he is able to reach) using the multipath propagation model which gives the same position as the measured data from the GNSS receiver. If this succeeds, the position obtained from the model is identical to the actual user's position. For speeding up calculations, the interval halving method can be used, repeating iterations in so many steps until an agreement between measured and calculated parameters is reached.

Detailed description of individual steps can be found in chapter 2 and chapter 5.

5. RESULTS

In this section, the method evaluation and results are presented. The ray-tracing algorithm is generally designed for different combinations of GNSS constellations – GPS, GLONASS, Galileo and Compass.

Different GNSS systems use different reference frames and different reference time scales for their positioning and timing solution. Therefore for each system, a matrix transforming satellite coordinates of a given GNSS system into the mapping coordinates has to be performed.

directional vectors of all lines and planes are described by matrixes.

Calculation of Single Reflection Length

Given by known coordinates of S, R_1 and P (as in Figure 4. 2), the reflection length for a single reflection can be simply calculated as:

$$D = d_1 + d_2, \tag{4. 20}$$

where d_1 is $|PR_1|$, and d_2 is $|SR_1|$ in meters.

As in the equation (4. 2), the distances d_1 and d_2 are calculated as:

$$d_1 = \sqrt{(R_{1x} - P_x)^2 + (R_{1y} - P_y)^2 + (R_{1z} - P_z)^2}, \tag{4. 21}$$

$$d_2 = \sqrt{(R_{1x} - S_x)^2 + (R_{1y} - S_y)^2 + (R_{1z} - S_z)^2}. \tag{4. 22}$$

From the knowledge that GNSS signals travel at the speed of light and the known distance to the receiver, we can simply calculate the time the signal took to reach the receiver.

The benefit of a single reflection is that after reflection, the circular polarization of a GNSS signal is changed to left-handed (LHCP). An RHCP antenna can supress the LHCP reflection quite effectively so the multipath reflection error is minimised. Naturally, a second reflection will cause the RHCP polarization again [17], [18], [19].

Calculation of multiple reflections length

The distance for multiple reflections, i.e. three points of reflection (Figure 4. 3), can be simply calculated as:

$$D = d_1 + d_2 + d_3 + d_4, \tag{4. 23}$$

where d_1 is $|PR_3|$, d_2 is $|R_2R_3|$, d_3 is $|R_1R_2|$, and d_4 is $|SR_1|$ in meters. S, R_1, R_2, R_3 and $\mathrm{P} \in R^3$ and their coordinates are known.

As in equation (4. 2), the distances d_1, d_2, d_3 and d_4 are calculated as:

$$d_1 = \sqrt{(R_{3x} - P_x)^2 + (R_{3y} - P_y)^2 + (R_{3z} - P_z)^2}, \tag{4. 24}$$

$$d_2 = \sqrt{(R_{3x} - R_{2x})^2 + (R_{3y} - R_{2y})^2 + (R_{3z} - R_{2z})^2}, \tag{4. 25}$$

$$d_3 = \sqrt{(R_{2x} - R_{1x})^2 + (R_{2y} - R_{1y})^2 + (R_{2z} - R_{1z})^2}, \tag{4. 26}$$

$$d_4 = \sqrt{(R_{1x} - S_x)^2 + (R_{1y} - S_y)^2 + (R_{1z} - S_z)^2}. \tag{4. 27}$$

where $R_1, A, B, C \in R^3$; $\alpha_1, \alpha_2, \alpha_3 \in R$. In other words, the point R_1 has to be a convex combination of the $\triangle$ABC.

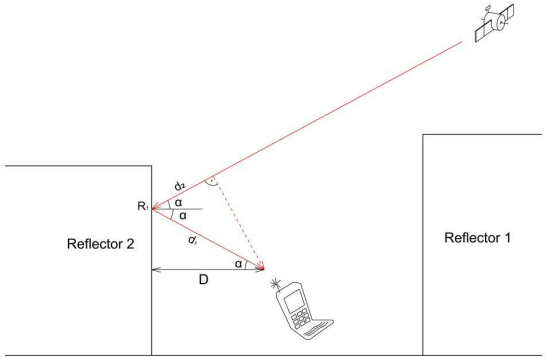

Figure 4. 2 Illustration of single reflection on a planar reflector

Given the point R_1 and the $\triangle$ABC, we find the solution to $\alpha_1, \alpha_2, \alpha_3$:

$$\mathbf{M}_{\alpha_1,\alpha_2,\alpha_3} = \left[\begin{array}{ccc|c} 1 & 1 & 1 & 1 \\ A_x & B_x & C_x & R_{1x} \\ A_y & B_y & C_y & R_{1y} \\ A_z & B_z & C_z & R_{1z} \end{array}\right]. \tag{4. 10}$$

To determine whether the intersection point R_1 does or does not lie inside the $\triangle$ABC, the algorithm verifies the conditions described in equation (4. 7), equation (4. 8) and gives the solution.

Single reflection path - one point of reflection

The equation for the plane ABC going through the point A is as [16]:

$$w_x A_x + w_y A_y + w_z A_z + d = 0, \tag{4. 11}$$

where $\mathbf{w}$ is the normal vector for the plane ABC defined in equation (4. 3).

It is assumed that the reflected point R_1 is part of lines $|SR_1|$ (defines the distance from the satellite S to the reflected point R_1), $|R_1P|$ (defines the distance from the reflected point R_1 to the known position of the receiver), and the plane ABC. Its coefficients are described by the normal vector $\mathbf{w}$.

Therefore, any reflected point R_1 on the plane ABC satisfies the normal implicit equation:

$$\mathbf{w}\cdot(\mathbf{R_1}-\mathbf{A})=0, \quad (4.\ 12)$$

and as in equation (4. 5), the reflection point R_1 can be expressed also by:

$$\mathbf{S}+\mathbf{n_1}\cdot t_1=\mathbf{P}+\mathbf{n_2}\cdot t_2, \quad (4.\ 13)$$

where S defines the known satellite position, P represents the assumed position of the receiver, $t_1, t_2 \in R$, $\mathbf{n_1}$ is the directional vector of the line $|SR_1|$, $\mathbf{n_2}$ is the directional vector of the line $|R_1P|$.

The relation between these two directional vectors is given by:

$$\mathbf{n_2}=\mathbf{n_1}\times\mathbf{M_{REF}}, \quad (4.\ 14)$$

where $\mathbf{M_{REF}}$ is the matrix describing reflection:

$$\mathbf{M_{REF}}=-inv\begin{bmatrix}\mathbf{w}\\ \mathbf{A}-\mathbf{B}\\ \mathbf{A}-\mathbf{C}\end{bmatrix}*\begin{bmatrix}-1&0&0\\0&1&0\\0&0&1\end{bmatrix}*\begin{bmatrix}\mathbf{w}\\ \mathbf{A}-\mathbf{B}\\ \mathbf{A}-\mathbf{C}\end{bmatrix}. \quad (4.\ 15)$$

Now we know whether there is a path with a single reflection between the satellite and the receiver. If so, the algorithm gives coordinates (X, Y, Z) of the reflected point $R_1 \in R^3$ as a result.

Calculation of Multiple Reflections

GNSS availability in urban environment is seriously degraded by buildings blocking direct signals from more than one side, as illustrated in Figure 4. 3.

Two reflections path – two points of reflection

Now when we know the reflection matrix, we can simply calculate if a GNSS signal arrived at the receiver via more than one reflection. The principle is similar: for the second reflection, the plane $A_2B_2C_2$, with normal vector $\mathbf{w_2}$ is defined.

The equation for the plane $A_2B_2C_2$ going through the point A_2 is as [16]:

$$w_{2x}A_{2x}+w_{2y}A_{2y}+w_{2z}A_{2z}+d_2=0. \quad . \quad (4.\ 16)$$

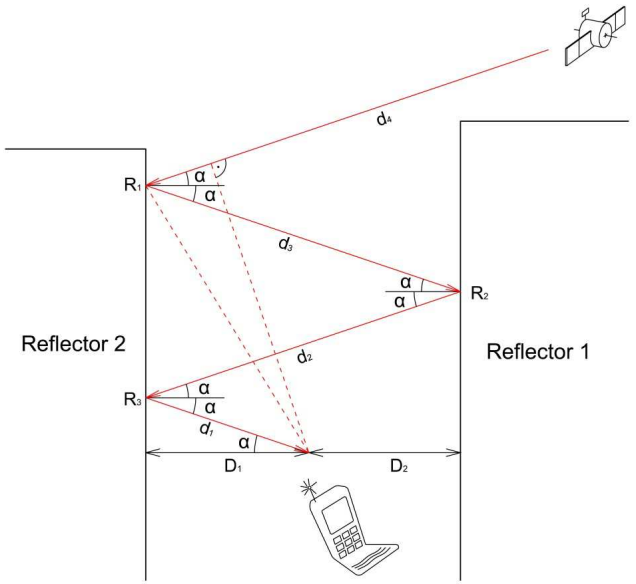

Figure 4. 3 Illustration of multiple reflections in planar reflectors

Similar to the equation (4. 5), the second reflection point R_2 can be expressed by:

$$\mathbf{R_1}+\mathbf{n_2}.t_2=\mathbf{P}+\mathbf{n_3}.t_3, \quad (4.\ 17)$$

where $t_2, t_3 \in R$, $\mathbf{n_2}$ is the directional vector of the line $|PR_2|$, $\mathbf{n_3}$ is the directional vector of the line $|R_2P|$.

The relation between the directional vectors $\mathbf{n_3}$ and $\mathbf{n_1}$ is given by:

$$\mathbf{n_3}=\mathbf{n_1}\times\mathbf{M_{2\_REF}}, \quad (4.18)$$

where $\mathbf{M_{REF}}$ is the matrix describing the first reflection, $\mathbf{M_{2\_REF}}$ is the matrix describing the second reflection:

$$\mathbf{M_{2\_REF}}=\mathbf{M_{REF}}*\left[-inv\begin{bmatrix}\mathbf{w_2}\\ \mathbf{A_2}-\mathbf{B_2}\\ \mathbf{A_2}-\mathbf{C_2}\end{bmatrix}*\begin{bmatrix}-1&0&0\\0&1&0\\0&0&1\end{bmatrix}*\begin{bmatrix}\mathbf{w_2}\\ \mathbf{A_2}-\mathbf{B_2}\\ \mathbf{A_2}-\mathbf{C_2}\end{bmatrix}\right]. \quad (4.\ 19)$$

For more reflections, the principle is the same. Generally, every side of a building is defined by a plane with a normal vector. This normal vector describes every point on a plane, therefore also the reflected point. Relations between